Zeitschrift: IABSE reports of the working commissions = Rapports des commissions de travail AIPC = IVBH Berichte der Arbeitskommissionen

Band: 34 (1981)

Artikel: 3-dimensional nonlinear analysis of reinforced concrete columns

Autor: Muto, Kiyoshi / Sugano, Tadashi / Miyashita, Takashi

DOI: https://doi.org/10.5169/seals-26903

3-Dimensional Nonlinear Analysis of Reinforced Concrete Columns

Analyse 3-dimensionnelle non-linéaire de colonnes en béton armé

3-Dimensionale nichtlineare Berechnung von Stahlbetonstützen

KIYOSHI MUTO
Professor Emeritus
University of Tokyo
Tokyo, Japan

TADASHI SUGANO
Dr. Eng., Senior Research Eng.
Muto Institute of Kajima Corp.
Tokyo, Japan

TAKASHI MIYASHITA
Senior Research Eng.

NORIO INOUE
Senior Research Eng.

SUMMARY
Experimental and analytical studies are presented on the nonlinear behavior of reinforced concrete columns under earthquake loads. The analytical method is based on the 3-dimensional Finite Element Method which enables dealing with repeated load reversals. To establish the nonlinear parameters of concrete, experiments and their simulation analyses of columns under axial force only were conducted with attention given to the confinement effect of hoops (ties). Finally a simulation analysis of a hooped column under repeated lateral forces and axial forces was conducted.

RÉSUMÉ
Le comportement non-linéaire des colonnnes en béton armé pour des charges sismiques est étudié au moyen de la Méthode des Eléments Finis Tri-dimensionnels, qui peut également être utilisée pour des charges répétées réversibles. Dans la première partie, des expériences et des analyses de simulation des colonnes portant uniquement la force axiale se sont conduit pour déterminer le paramètre non-linéaire du béton en tenant compte du faible effet des étriers. Ensuite l'analyse de simulation de la colonne avec étriers portant les forces latérales et axiales est faite.

ZUSAMMENFASSUNG
Das nichtlineare Verhalten von Stahlbetonstützen unter Erdbebenbelastung ist mit 3-dimensionaler Finite-Elemente-Methode untersucht, die eine Behandlung der Wechselbelastung ermöglicht.
Am Anfang wurden Versuch und simulierende Analysis der Stützen nur mit der Axialkraft durchgeführt, um die nichtlinearen Parameter des Betons unter Berücksichtigung der Umschliessungswirkung der Bügel festzusetzen.
Dann wurde die simulierende Analysis von Stützen mit Bügelbewehrung unter Wechselbelastung und Axialkraft durchgeführt.

1. INTRODUCTION

When a reinforced concrete column is subjected to repeated lateral forces, such as earthquake loads, its plastic behavior is considerably influenced not only by longitudinal reinforcement but also by lateral reinforcement, which confines core concrete. This paper presents a study of the three dimensional nonlinear behavior of reinforced concrete columns by experiments and analyses, with attention given to afore-mentioned confining effect (1).

In the proposed method of analysis a reinforced concrete column is considered to be composed of core concrete, cover concrete, reinforcing bars and bonds with appropriate nonlinearity of each element. For core concrete the plasticity theory assuming Drucker-Prager's yield function is adopted as it is a simple formula which can introduce the volume dilatancy caused by the plastic deformation of concrete. Further hysteretic loops are assumed for each element so that the reversal of loading can be analyzed.

In the beginning experiments and their simulation analyses of columns subjected to axial force only were conducted to establish the nonlinearity parameter with attention given to the confinement effect of hoops.

Then the proposed method was applied to a column subjected to repeated lateral forces and axial force. This pursued the reversal of loading from the positive to the negative region.

2. METHOD OF ANALYSIS

2.1 Modeling of column

A reinforced concrete column is considered to be composed of core concrete, cover concrete, longitudinal and lateral reinforcing bars, and bond between concrete and reinforcing bars as shown in Fig. 1 (2,3,4). Here core concrete and cover concrete are modeled separately because the former shows improvement of strength and ductility compared with the latter. Such behavior is caused by the confinement effect of lateral reinforcement, which can be investigated only by these three dimensional studies.

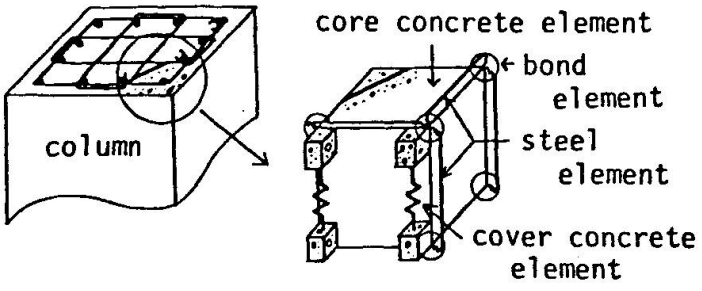

Fig. 1 Modeling of Column

2.2 Core concrete element

2.2.1 Modeling of core concrete

Core concrete is represented by a hexahedral isoparametric element (5). For numerical integration two integrating points are assumed in each direction and Gaussian Quadrature Formula is adopted. The nonlinearity of concrete is judged by the stress and strain at eight Gauss points respectively.

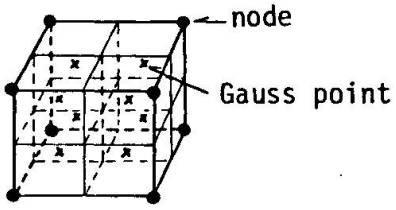

Fig. 2 Core Concrete Element

2.2.2 Nonlinearity in compressive side

The constitutive equation of concrete in plastic range is defined by several theories, such as plasticity [6,7], nonlinear elasticity [8,9,10,11], orthotropic model [12,13,14], Endochronic theory [15] and others [16,17]. Among them the plasticity theory is adopted in this analysis. Then the nonlinearity of concrete is defined by the initial yield condition, flow rule and hardening rule as indicated below. The constants adopted in their rules are established to be adequate to uniaxial condition. Next the first yield surface and the second one are considered homologous and the ultimate strain is replaced with the ultimate equivalent plastic strain.

Initial yield condition: For the yielding criteria of concrete, several functions are proposed [18,19,20,21]. As a matter of course, if more parameters are assumed, better coincidence will be obtained. In this analysis the following Drucker-Prager's function is adopted as it is the simplest formula which can introduce the volume dilatancy caused by the plastic deformation of concrete. Then only one parameter α is assumed for representing the nonlinearity of concrete.

$$f = \frac{3}{2}\alpha(\sigma_x+\sigma_y+\sigma_z)+f_0 = k \tag{1}$$

$$f_0^2 = \frac{1}{2}\{(\sigma_y-\sigma_z)^2+(\sigma_z-\sigma_x)^2+(\sigma_x-\sigma_y)^2+6(\tau_{yz}^2+\tau_{zx}^2+\tau_{xy}^2)\} \tag{2}$$

Where k is a constant representing strength of concrete, which is obtained by the uniaxial test. This yield function can be shown by principal stress field as in Fig. 3.

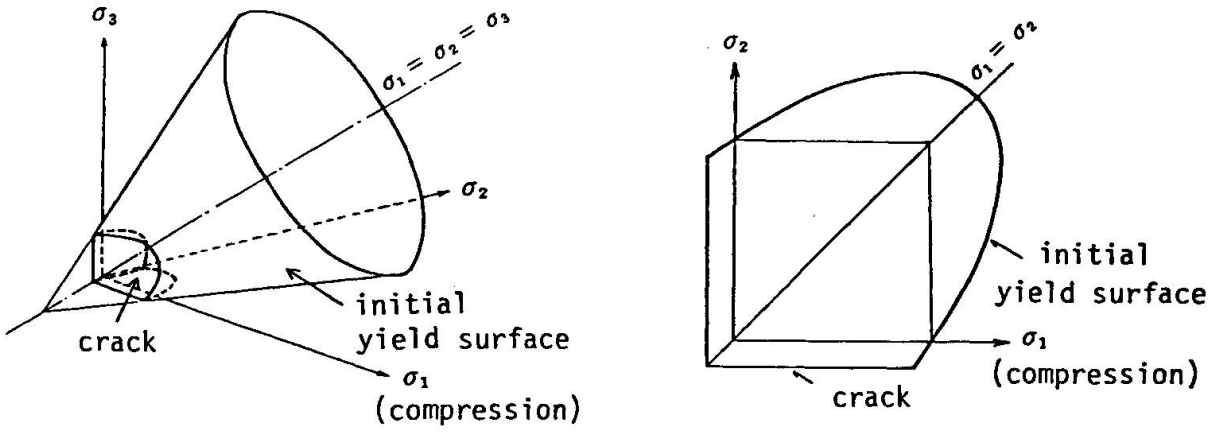

(A) 3 Dimension (B) 2 Dimension

Fig. 3 Initial Yield Condition

Flow rule: Due to v. Mises the plastic strain increment vector $\{d\varepsilon^p\}$ lies in the exterior normal of the yield surface at the stress point (Fig. 4).

$$\{d\varepsilon^p\} = \left\{\frac{\partial f}{\partial \sigma}\right\} d\lambda \qquad d\lambda > 0 \tag{3}$$

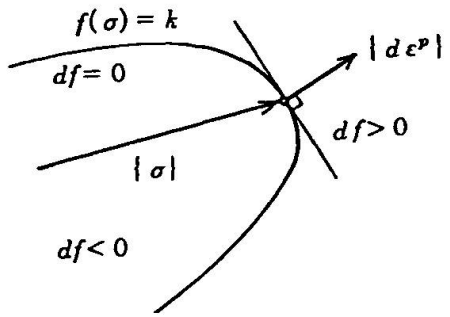

Fig. 4 Flow Rule

Hardening rule: Prager's kinematic hardening rule modified by Ziegler [22] is used (Fig. 5). The incremental translation of the center of the yield surface $\{d\sigma_0\}$ is defined by

$$\{d\sigma_0\} = \{\sigma - \sigma_0\}\, d\mu \qquad d\mu > 0 \tag{4}$$

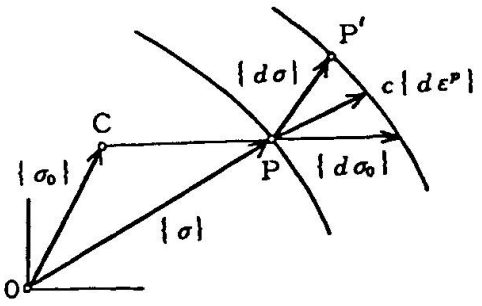

Fig. 5 Hardening Rule

Here the yield surface moves in the direction of the vector CP connecting the center of the yield surface with the stress point. The scalar $d\mu$ in Eq. 4 is determined by the condition that P remains on the yield surface in plastic flow. This condition is

$$\{d\sigma - d\sigma_0\}^T \left\{\frac{\partial f}{\partial \sigma}\right\} = 0 \tag{5}$$

and from Eq. 4 and Eq. 5 the following is obtained.

$$d\mu = \frac{\left\{\frac{\partial f}{\partial \sigma}\right\}^T \{d\sigma\}}{\{\sigma - \sigma_0\}^T \left\{\frac{\partial f}{\partial \sigma}\right\}} \tag{6}$$

If it is assumed that the vector $c\{d\varepsilon^p\}$ is the projection of $\{d\sigma\}$ (and thus of $\{d\sigma_0\}$) on the exterior normal of the yield surface, this condition is

$$\{d\sigma - c\, d\varepsilon^p\}^T \left\{\frac{\partial f}{\partial \sigma}\right\} = 0 \tag{7}$$

then from Eq. 3 and Eq.7 the following is obtained.

$$d\lambda = \frac{1}{c} \frac{\left\{\frac{\partial f}{\partial \sigma}\right\}^T \{d\sigma\}}{\left\{\frac{\partial f}{\partial \sigma}\right\}^T \left\{\frac{\partial f}{\partial \sigma}\right\}} \tag{8}$$

Constitutive equation of concrete: The stress vs. strain relation in elastic range is represented incrementally by the Hooke's law.

$$\{d\sigma\} = [D^e]\{d\varepsilon^e\} \tag{9}$$

The total strain is obtained by the summation of elastic strain and plastic strain.

$$\{d\varepsilon\} = \{d\varepsilon^e\} + \{d\varepsilon^p\} \tag{10}$$

Then from Eq. 3 through Eq. 10 the constitutive equation in plastic range is represented by

$$\{d\sigma\} = [D^p]\{d\varepsilon\}$$

$$= \left[[D^e] - \frac{[D^e]\left\{\frac{\partial f}{\partial \sigma}\right\}\left\{\frac{\partial f}{\partial \sigma}\right\}^T [D^e]}{c\left\{\frac{\partial f}{\partial \sigma}\right\}^T \left\{\frac{\partial f}{\partial \sigma}\right\} + \left\{\frac{\partial f}{\partial \sigma}\right\}^T [D^e] \left\{\frac{\partial f}{\partial \sigma}\right\}} \right] \{d\varepsilon\} \tag{11}$$

Crush: When the equivalent plastic strain $\bar{\varepsilon}^p$ reaches the limited value, crush is considered to occur. After that all stresses sustained by concrete are released.

$$\bar{\varepsilon}^p = -\frac{\sqrt{2}}{3}\{(\varepsilon_y^p - \varepsilon_z^p)^2 + (\varepsilon_z^p - \varepsilon_x^p)^2 + (\varepsilon_x^p - \varepsilon_y^p)^2 + 1.5(\gamma_{yz}^{p2} + \gamma_{zx}^{p2} + \gamma_{xy}^{p2})\}^{\frac{1}{2}} \tag{12}$$

If crush occurs at the j Gauss point in i concrete element, stresses $\{\sigma_i^j\}$ are transformed into equivalent nodal forces $\{F_i^j\}$.

$$\{\varepsilon_i\} = [B_i]\{\delta_i\} \tag{13}$$

$$\{F_i^j\} = \iiint [B_i]^T \{\sigma_i^j\} dV \tag{14}$$

Where $\{\varepsilon_i\}$ and $\{\delta_i\}$ are strain and nodal displacement of i element respectively.

2.2.3 Nonlinearity in tensile side

When the maximum principal stress reaches the tensile strength, the cracking is assumed to occur along a plane normal to the principal stress direction. Accordingly, the stresses in the direction are released and transformed into equivalent nodal forces just as in the method described above. Cracking is judged at each Gauss point, where three cracks can occur and they are mutually orthogonal. After cracking the shear transfer factor along the

cracked surface is reduced to β. This reducing factor should be a function of the gap between crack surfaces, but in this analysis it is assumed to be a constant value from 0 to 1.

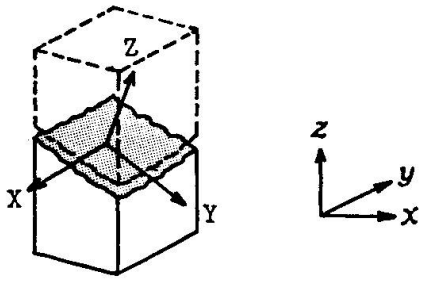

Fig. 6 Concrete Element after Cracking

After cracking, if the local co-ordinates X-Y-Z are defined according to the crack surface, the constitutive equation is represented as the following in local co-ordinates. Here the elements d_{ij}^{p} are calculated by solving a two dimensional problem in X-Y co-ordinates just like three dimensional one. This stiffness matrix is transformed by rotation matrix into the matrix defined in global co-ordinates.

$$\begin{Bmatrix} d\sigma_X \\ d\sigma_Y \\ d\sigma_Z \\ d\tau_{YZ} \\ d\tau_{ZX} \\ d\tau_{XY} \end{Bmatrix} = \begin{bmatrix} d_{11}^{p} & d_{12}^{p} & 0 & 0 & 0 & d_{13}^{p} \\ d_{21}^{p} & d_{22}^{p} & 0 & 0 & 0 & d_{23}^{p} \\ 0 & 0 & 0 & 0 & 0 & 0 \\ 0 & 0 & 0 & \beta G & 0 & 0 \\ 0 & 0 & 0 & 0 & \beta G & 0 \\ d_{31}^{p} & d_{32}^{p} & 0 & 0 & 0 & d_{33}^{p} \end{bmatrix} \begin{Bmatrix} d\varepsilon_X \\ d\varepsilon_Y \\ d\varepsilon_Z \\ d\gamma_{YZ} \\ d\gamma_{ZX} \\ d\gamma_{XY} \end{Bmatrix} \tag{15}$$

2.2.4 Hysteretic loop

The hysteretic loop of concrete is defined as the tri-linear curve which is expressed under uniaxial force (Fig. 7). Below the first yielding point the concrete remains elastic and after that it is semi-elastic up to the second yielding point. After the second point the tangent stiffness modulus is assumed very small and crush occurs when the strain reaches the limited value. In reversal region the usual tri-linear one is adopted.

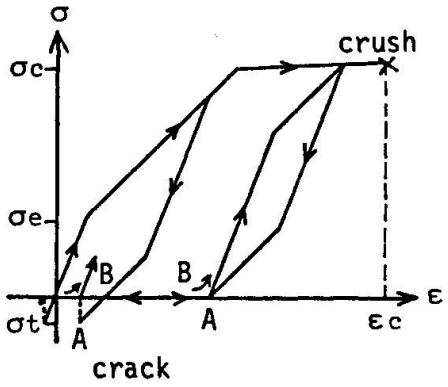

Fig. 7 Hysteretic Loop of Core Concrete

When the stress reaches the tensile strength, cracking occurs at point A. Thereafter if the strain returns to point B (where the cracking occurred in the former stage), the concrete revives elasticity. But the tensile stress normal to cracking surface is assumed not to be sustained.

2.3 Cover concrete, steel and bond elements

2.3.1 Cover concrete

This is represented by a rod element possessing only longitudinal stiffness. The stress vs. strain relation is characterized by the uniaxial state of concrete. The reduction of strength after the peak stress is considered as shown in Fig. 9. The hysteretic rule is assumed to be the same as core concrete.

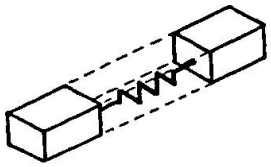

Fig. 8 Cover Concrete Element

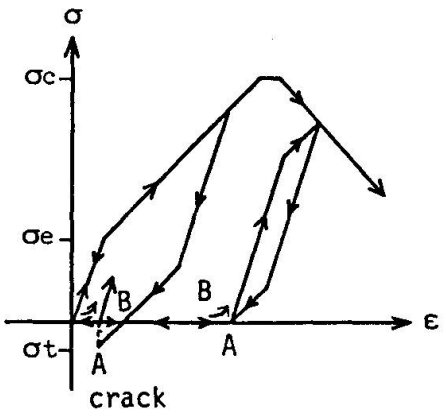

Fig. 9 Hysteretic Loop of Cover Concrete

2.3.2 Steel reinforcement

This is represented by a rod element possessing only axial stiffness. The stress vs. strain relation is assumed to be a bi-linear loop (Fig. 11).

Fig. 10 Steel Element

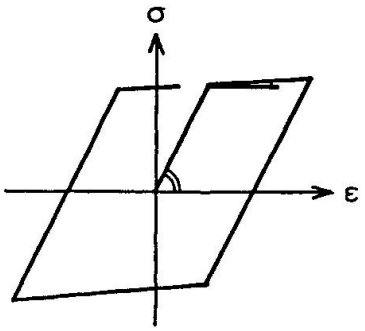

Fig. 11 Hysteretic Loop of Steel

2.3.3 Bonds

They are modeled as a set of link elements connecting steel elements and concrete elements. For bond force vs. relative displacement between steel and concrete elements, a slip-type bi-linear loop is assumed (Fig. 13).

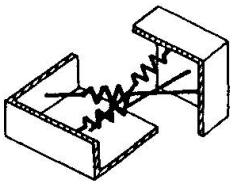

Fig. 12 Bond Element

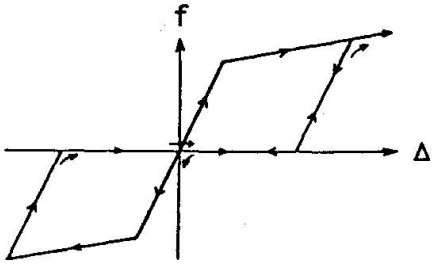

Fig. 13 Hysteretic Loop of Bond

3. PROCEDURE OF CALCULATION

The equilibrium equation is solved incrementally by step by step method. Nonlinearity or revival of elasticity is checked by obtained stress and strain in each element, and the alteration of stiffness is executed if necessary. The procedure is shown in Fig. 14.

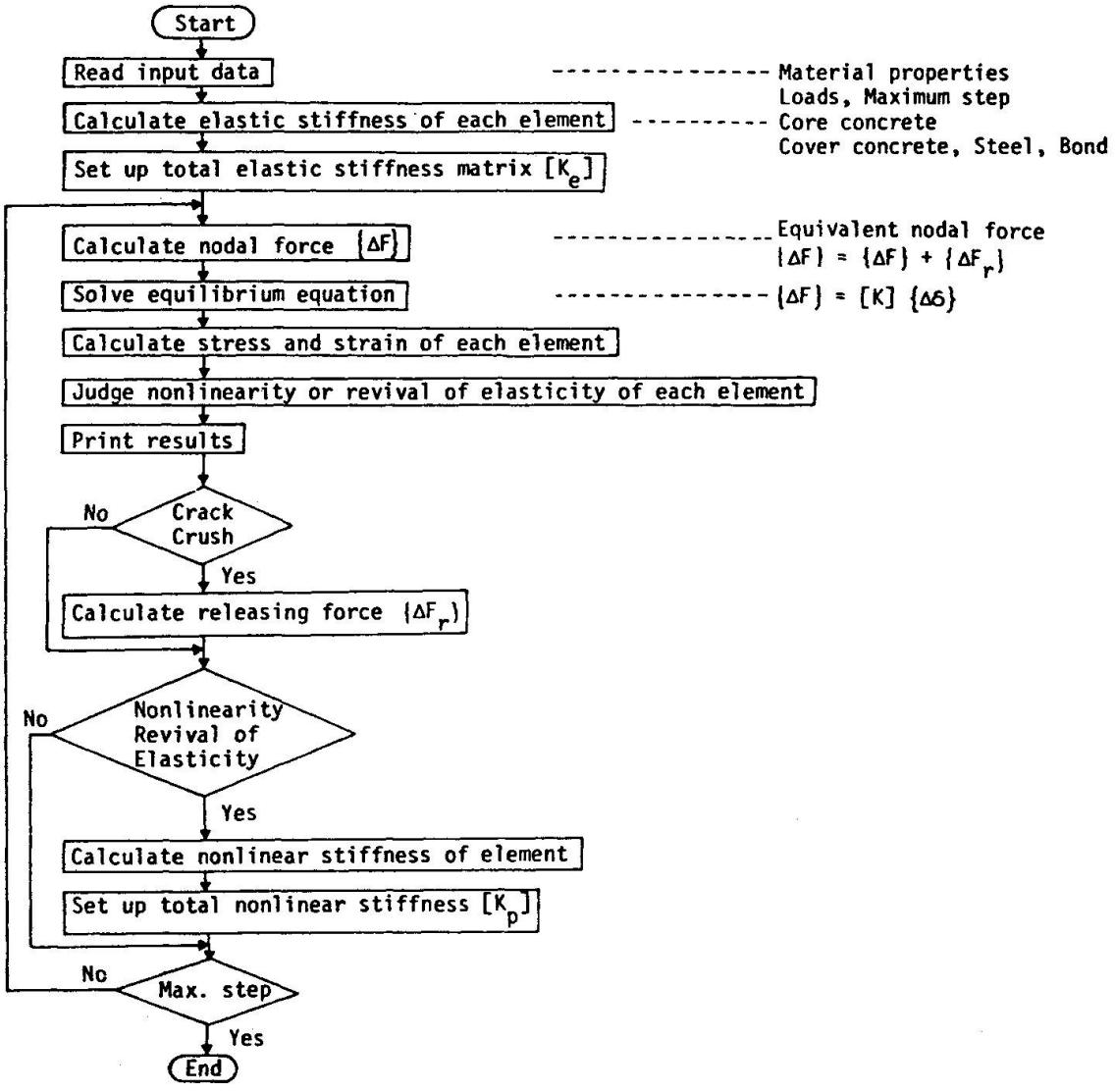

Fig. 14 Flow Chart of Calculation

4. EXPERIMENT AND ANALYSIS TO DETERMINE α

4.1 Purpose

Experiments and their simulation analyses of columns subjected to axial force only were conducted to establish the nonlinear parameter α of concrete in the Drucker-Prager's function. This is the simplest application model for a reinforced concrete column, which can be said to mean the compressive side of a column subjected to earthquake loads.

Many researchers have conducted these experiments and have pointed out the improvement of strength and ductility of confined concrete [23,24,25,26,27]. The authors investigated this confinement effect and determined α.

4.2 Outline of experiment

The test specimen is a column with square hoops which is 45 cm long and cross sectional dimensions of 18 cm x 18 cm (Fig. 15, Photo. 1). The diameter of hoops is 6 mm and their spacing is 20 mm. So the ratio of lateral reinforcement is 1.57%. Normal concrete is used and its compressive strength obtained by the cylinder test is 200 kg/cm^2.

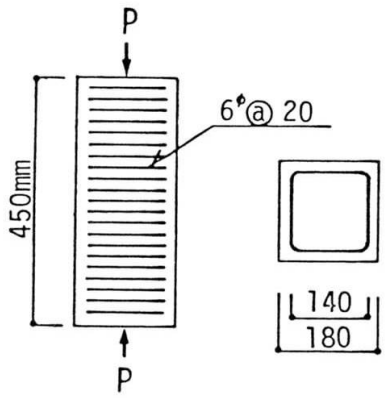

Fig. 15 Section of Test Specimen

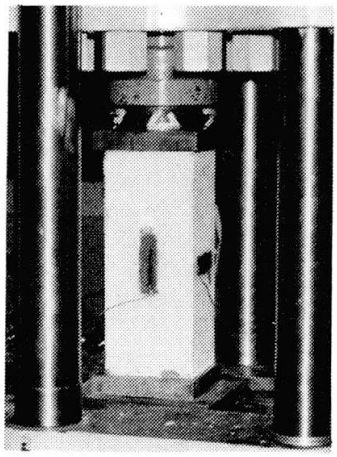

Photo. 1 Test Specimen

The vertical and lateral strain of concrete were measured at the surface in the middle of the specimen to exclude confining effect caused by the loading boundary. The strain of a hoop located in the middle of the column was measured at its center and end portion. These strains were measured at inside and outside surface to exclude bending component (Fig. 16).

Loading cycles are as follows. First axial loads were gradually increased up to 60 ton and then reversed to zero. Next they were increased up to the first peak value 77.9 ton and decreased to 50 ton. Finally they were increased up to the next peak value 80.3 ton, when the forces were sustained only by core concrete as the cover concrete broke away.

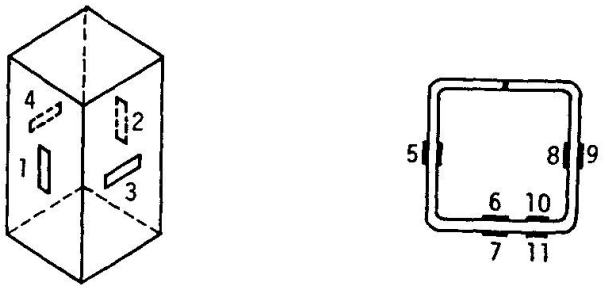

(A) Concrete (B) Hoop

Fig. 16 Measurement of Strain

4.3 Results of experiment

The observed vertical strain of concrete and strain of hoops are shown in Fig. 17 (A) and (B) respectively. In these figures the solid lines are observed results at inside and outside, and the broken lines are their mean values excluding bending component.

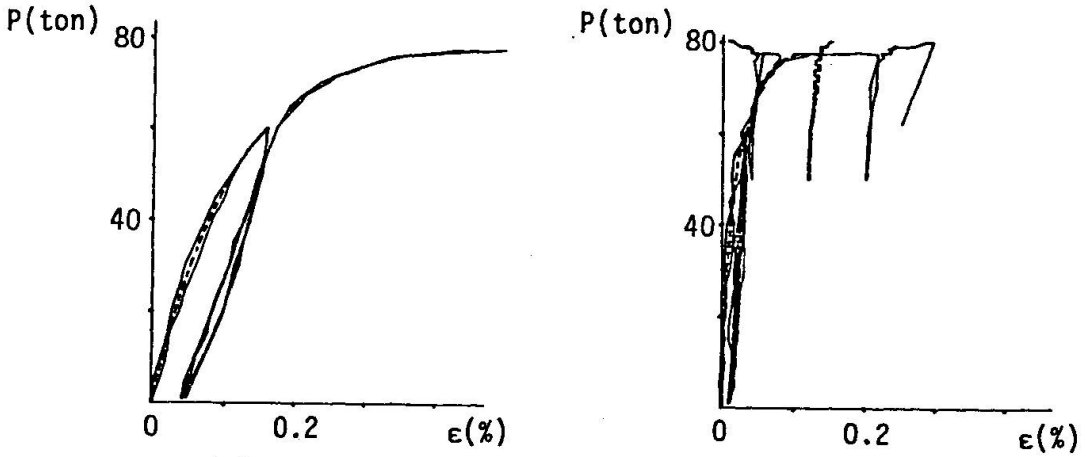

(A) Concrete (B) Hoop

Fig. 17 Observed Strain

4.4 Model for analysis

In Fig. 18 the model of core concrete for analysis is presented. Taking

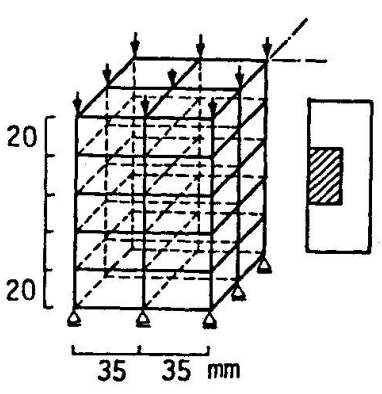

Fig. 18 Mesh Layout of Core Concrete

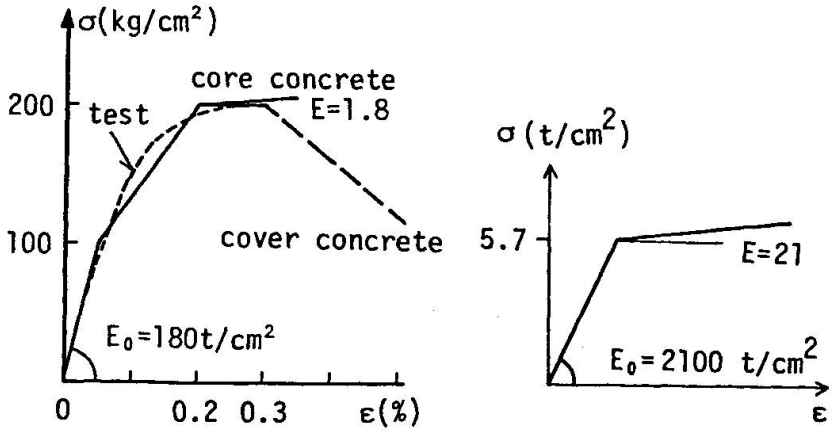

(A) Concrete (B) Steel

Fig. 19 Material Properties

advantage of the symmetrical condition one quarter portion was considered horizontally. Vertically five layers were adopted to decrease the influence of boundary conditions. The hoops were assumed to be anchored to concrete at the corner and center of core concrete. Material properties used in this analysis are presented in Fig. 19. The parameter $3/2\,\alpha$ of concrete is assumed to be 0, 0.1, 0.2, 0.3 and 0.4.

4.5 Results of analysis

Loads vs. vertical strain of concrete is presented in Fig. 20. Here (A) shows the bearing forces of core concrete and cover concrete respectively. From this it is recognized that core concrete can sustain further force after the force of cover concrete has decreased as α increases due to the confinement effect of the hoops. In (B) the sum of the two values are compared with observed results. This shows that the maximum strength of a column is decided according to the sum of the ascending gradient of core concrete and the descending gradient of cover concrete. Among the calculated results the value obtained by assuming $3/2\,\alpha = 0.2$ shows best agreement.

Loads vs. strain of hoop is presented in Fig. 21. From this the effectiveness of hoops is recognized distinctly after the stress of concrete has reached the vicinity of compressive strength of plain concrete. In the case of hoops the best result is obtained also by assuming $3/2\,\alpha = 0.2$. Here it is noticeable that the hoops remain elastic when the column reaches the maximum value.

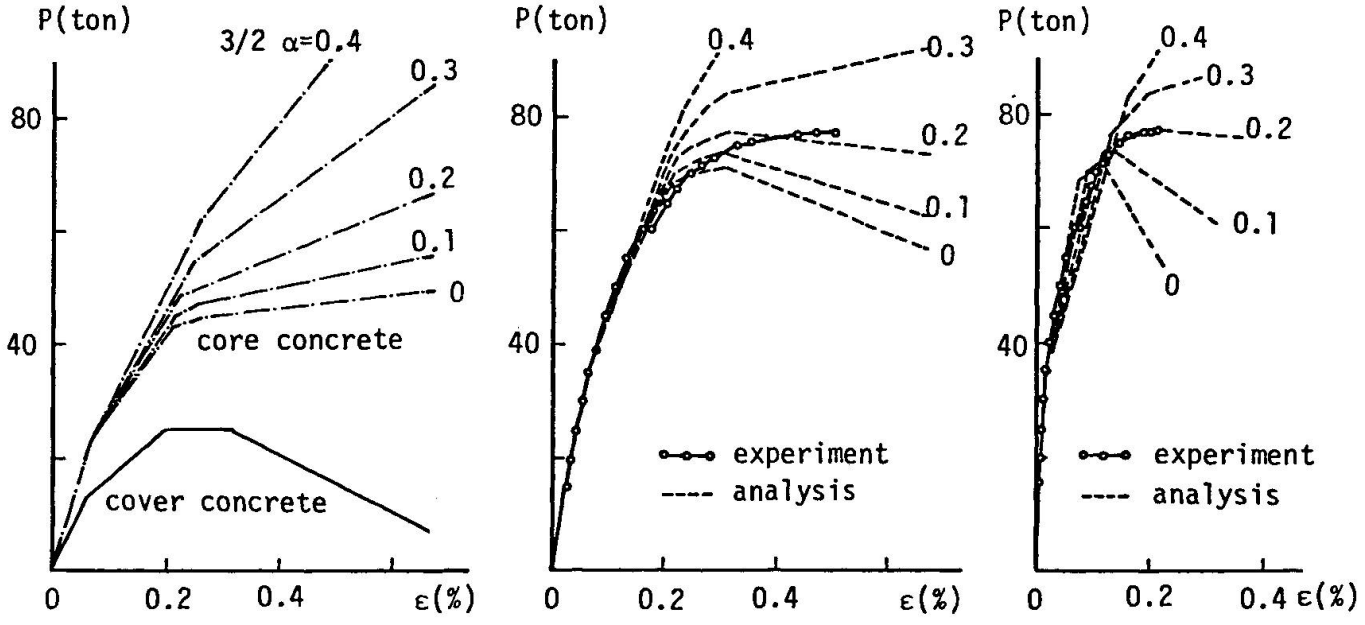

(A) Core and Cover Concrete (B) Total

Fig. 20 Loads vs. Vertical Strain of Concrete

Fig. 21 Loads vs. Strain of Hoop

5. ANALYSIS OF COLUMN UNDER REPEATED LATERAL FORCES

5.1 Outline of experiment

The test specimen is a 1/2 scaled column subjected to repeated lateral forces with a constant axial force which is equal to one third of compressive strength as shown in Fig. 22 (28). During the first and second cycles, the loading was gradually increased up to 30 tons and 60 tons respectively. Then 30 cycles of loading were applied to the specimen, keeping the maximum deflection constant at a relative deflection angle R of 1/100 rad. Finally, the relative deflection angle of the specimen was increased to 1/50 rad. In Fig. 23 and Fig. 24 the observed relative deflection and strain of longitudinal reinforcement are presented respectively.

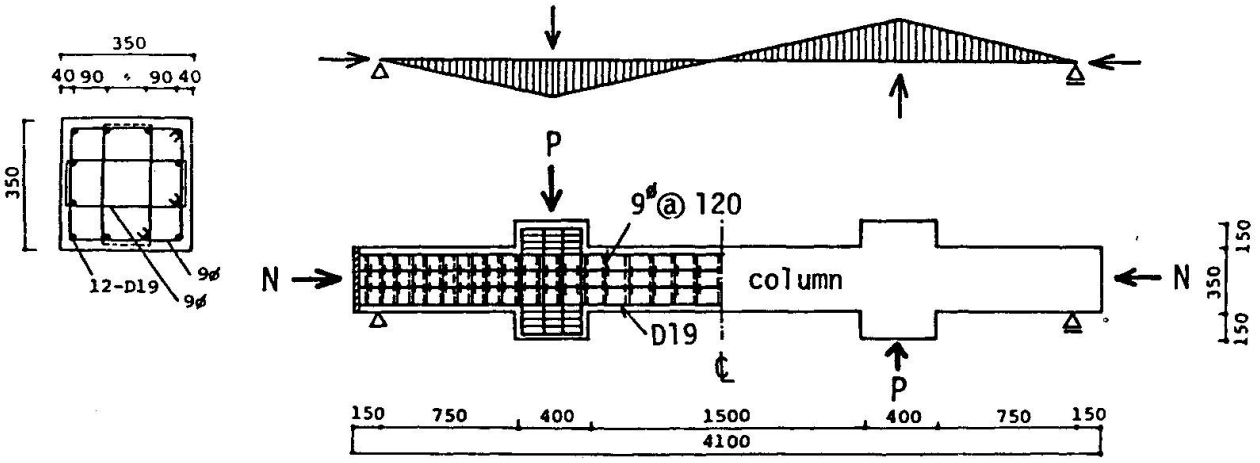

Fig. 22 Test Column (by Hisada, Ohmori and Bessho)

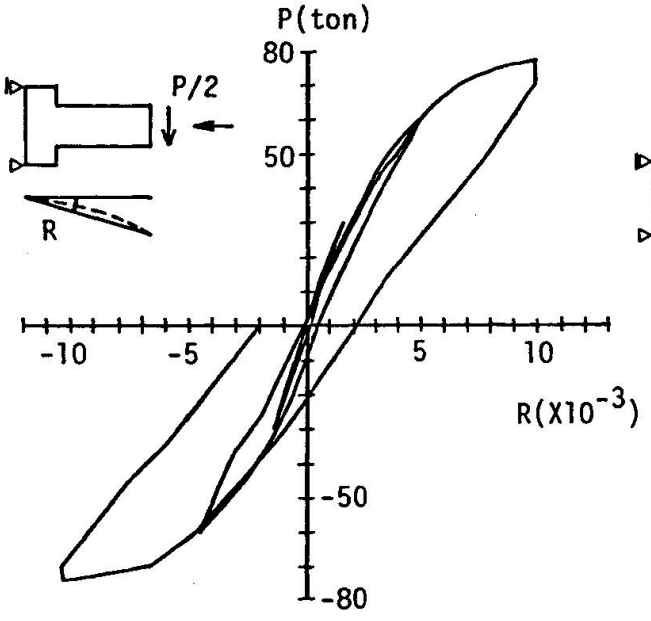

Fig. 23 Observed Relative Deflection

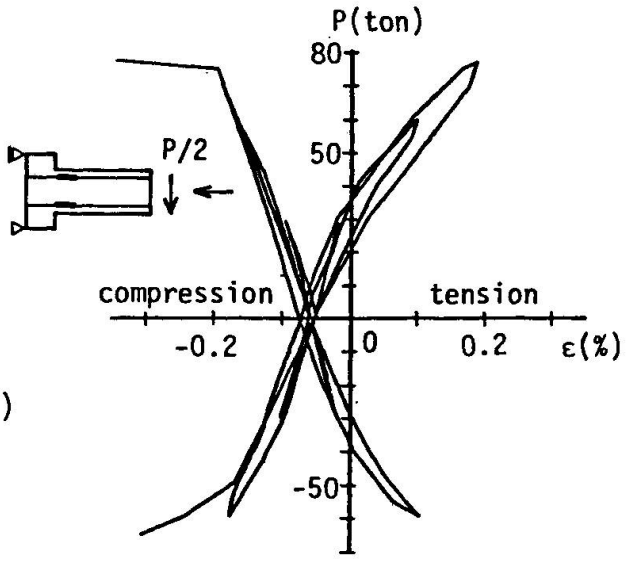

Fig. 24 Observed Strain of Longitudinal Reinforcement

5.2 Model for analysis

Analysis was performed on a half model by considering its antisymmetry (Fig. 25). The assumed material properties are shown in Tab. 1. Here, $3/2\,\alpha = 0.2$ is assumed from the result of the afore-mentioned preliminary study. The second and third loading cycles were simulated because the first one is considered elastic.

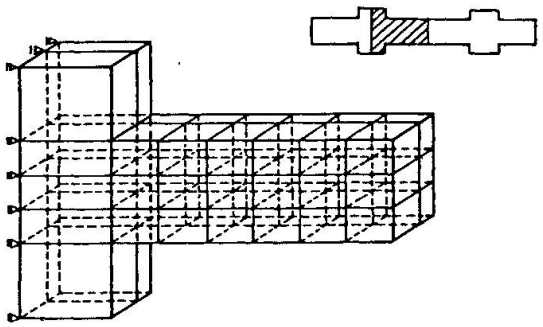

Fig. 25 Mesh Layout of Core Concrete

Tab. 1 Material Properties

Concrete

compressive strength	370 kg/cm²
elastic limit	133 kg/cm²
tensile strength	28 kg/cm²
elastic modulus	180 t/cm²
semi-elastic modulus	136 t/cm²
$3/2\alpha$	0.2
Poisson's ratio	0.2
limiting comp. strain	0.0035

Steel

yield stress	
longitudinal bar	3.7 t/cm²
transverse bar	3.6 t/cm²
Young's modulus	2100 t/cm²

Bond

yield stress	
longitudinal bar	50 kg/cm³
transverse bar	30 kg/cm³
first stiffness	25 t/cm³
second stiffness	0.84 t/cm³

5.3 Results of analysis

Among obtained results deflection and strain of longitudinal reinforcement are shown in Fig. 26 and Fig. 27 respectively. Here the second and third cycle are separately shown. The observed results are well simulated by this analysis from the positive to the negative region on the deflection and strain of longitudinal reinforcement. Especially, it is very important that the behavior while unloading is obtained by this incremental analysis method.

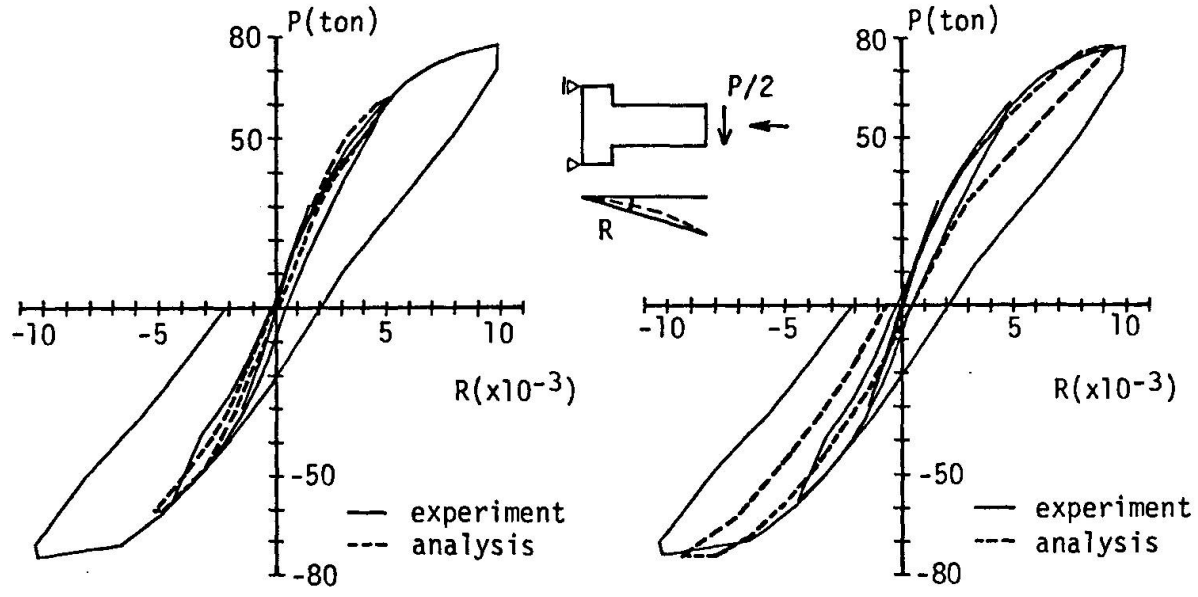

(A) 2nd Cycle (B) 3rd Cycle

Fig. 26 Relative Deflection

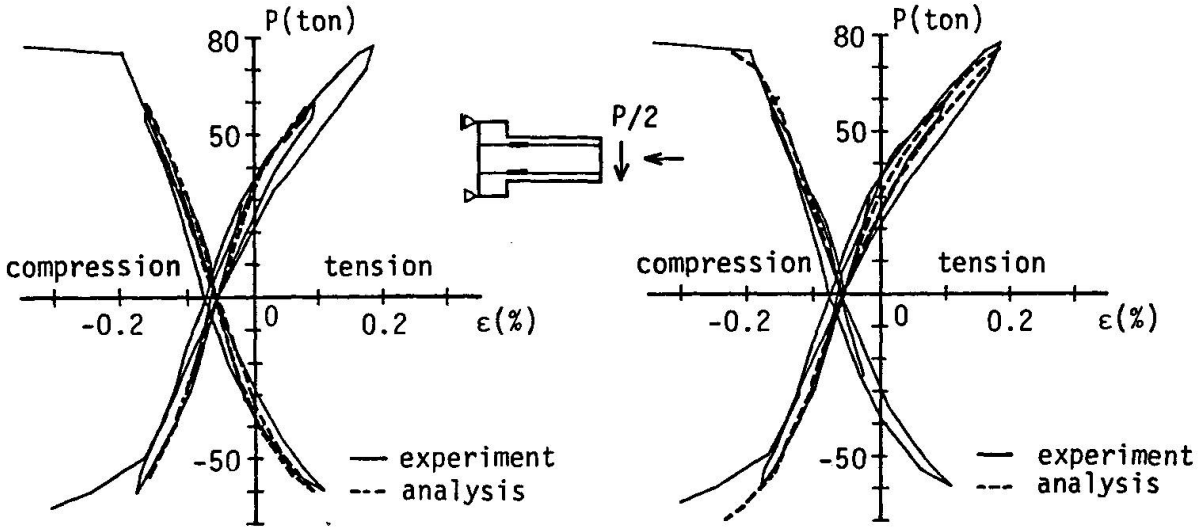

(A) 2nd Cycle (B) 3rd Cycle

Fig. 27 Strain of Longitudinal Reinforcement

Finally in Fig. 28 (A) and (B), the calculated axial stresses at the critical cross section are presented at the stage when the load is 70 and 76 ton respectively. Here the arrow marks mean forces of longitudinal bars and shaded zones mean axial stress distribution of concrete. It is noticeable in Fig. (B) that the maximum compressive stress of concrete occurs in core concrete by the confining effect of hoops.

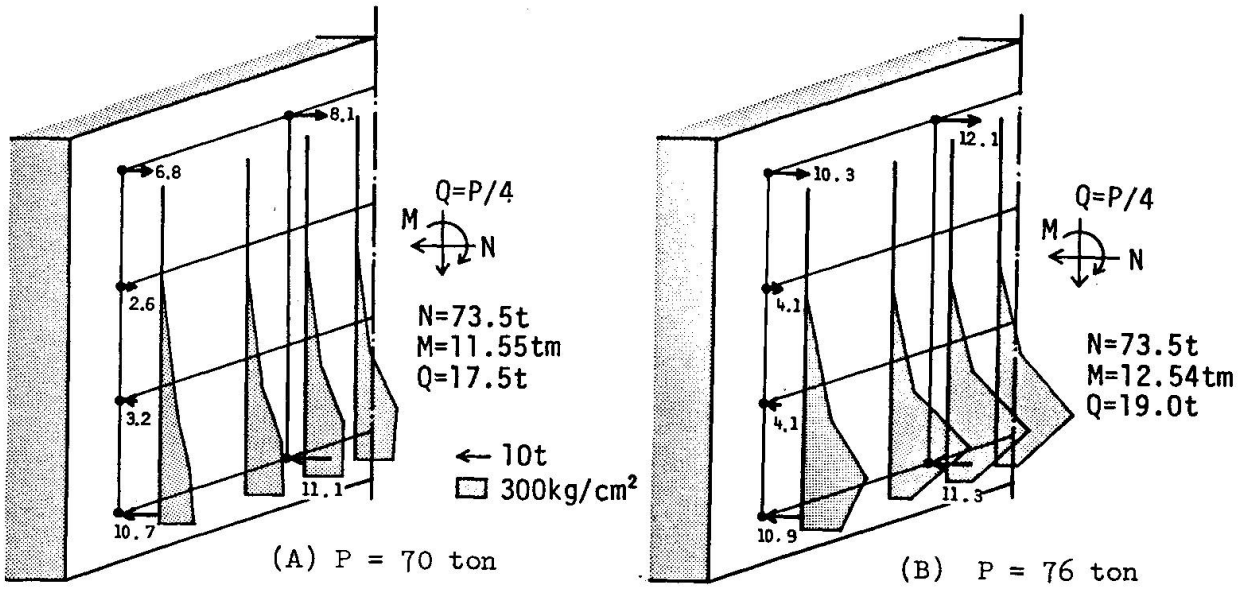

Fig. 28 Calculated Axial Stresses

6. CONCLUSION

The nonlinear behavior of reinforced concrete columns were studied by 3-dimensional Finite Element Method developed by the authors. First the preliminary study determined the parameter α used in plastic condition of concrete. Then, on the basis of these results, a simulation analysis of a hooped column under repeated lateral forces was performed from the positive to the negative region and good agreement was obtained.

7. ACKNOWLEDGMENTS

Y. Abe conducted the uniaxial test and S. Bessho provided the results of a hooped column subjected to repeated lateral forces. They are acknowledged with gratitude.

8. REFERENCES

1. Sugano, T., Miyashita, T., and Inoue, N., " 3-dimensional Study of Nonlinear Behavior of Reinforced Concrete Column under Repeated Lateral Forces," Proceedings of 7th World Conference on Earthquake Engineering, Vol.5, 1980, pp. 497-504
2. Ngo, D., and Scordelis, A.C., "Finite Element Analysis of Reinforced Concrete Beams," ACI Journal, Vol. 64, No. 3, March, 1967, pp. 152-163
3. Franklin, H.A., "Nonlinear Analysis of Reinforced Concrete Frames and Panels," Structures and Materials Research Department of Civil Engineering, University of California
4. Valliappan, S., and Doolan, T.F., "Nonlinear Stress Analysis of Reinforced Concrete," Journal of the Structural Division, ASCE, Vol. 98, No. ST4, 1972 pp. 885-897
5. Zienkiewicz, O.C., "The Finite Element Method in Engineering Science," McGraw-Hill, 1971.
6. Chen, A.C.T., and Chen, W.F., "Constitutive Equations and Punch-Indentation of Concrete," Journal of the Engineering Mechanics Division, ASCE, Vol.101, No. EM6, Dec., 1975, pp. 889-906
7. Suidan, M., and Schnobrich, W.C., "Finite Element Analysis of Reinforced Concrete," Journal of the Structural Division, ASCE, Vol. 99, No. ST10,

Oct., 1973, pp. 2109-2122
8. Kupfer, H., and Gerstle, K., "Behavior of Concrete Under Biaxial Stress," Journal of the Engineering Mechanics Division, ASCE, Vol. 99, No. EM4, Aug., 1973, pp. 852-866
9. Cedolin, L., Crutzen, R.J., and Poli, S.D., "Triaxial Stress-Strain Relationship for Concrete," Journal of the Engineering Mechanics Division, ASCE, Vol. 103, No. EM3, June, 1977, pp. 423-439
10. Palaniswamy, R., and Shah, S.P., "Fracture and Stress-Strain of Concrete Under Triaxial Compression," Journal of the Structural Division, ASCE, Vol. 100, No. ST5, May, 1974, pp. 901-916
11. Kotsovos, M.D., and Newman, J.B., "Generalized Stress-Strain Relations for Concrete," Journal of the Engineering Mechanics Division, ASCE, Vol. 104, No. EM4, Aug., 1978, pp. 845-856
12. Darwin, D., and Pecknold, D.A., "Inelastic Model for Cyclic Biaxial Loading of Reinforced Concrete," University of Illinois, UILU-ENG-74-2018, 1974
13. Elwi, A.A., and Murray, D.W., "A 3D Hypoelastic Concrete Constitutive Relationship," Journal of the Engineering Mechanics Division, ASCE, Vol. 105, No. EM4, Aug., 1979, pp. 623-641
14. Liu, T.C.Y., Nilson, A.H., and Slate, F.O., "Biaxial Stress-Strain Relations for Concrete," Journal of the Structural Division, ASCE, Vol. 98, No. ST5, May, 1972, pp. 1025-1034
15. Bažant, Z.P., Bhat, P.D., and Shieh, C.L., "Endochronic Theory for Inelasticity and Failure Analysis of Concrete Structures," Northwestern University, Structural Engineering Report, No. 1976-12/259, Dec., 1976
16. Romstad, K.M., Taylor, M.A., and Hermann, L.R., "Numerical Biaxial Characterization for Concrete," Journal of the Engineering Mechanics Division, ASCE, Vol. 100, No. EM5, Oct., 1974, pp. 935-948
17. Ottosen, N.S., "Constitutive Model for Short-Time Loading of Concrete," Journal of the Engineering Mechanics Division,ASCE, Vol. 105, No. EM1, Feb., 1979, pp. 127-141
18. Hobbs, D.W., Pomeroy, C.D., and Newman, J.B., "Design Stresses for Concrete Structures Subject to Multi-axial Stresses," The Structural Engineer, Vol. 55, No. 4, Apr., 1977
19. Kotsovos, M.D., "Effect of Stress Path on the Behavior of Concrete Under Triaxial Stress States," ACI Journal, Feb., 1979
20. Andenaes, E., Gerstle, K., and Ko, H.Y., "Response of Mortar and Concrete to Biaxial Compression," Journal of the Engineering Mechanics Division, ASCE, Vol. 103, No. EM4, Aug., 1977, pp. 515-526
21. Ottosen, N.S., "A Failure Criterion for Concrete," Journal of the Engineering Mechanics Division, ASCE, Vol. 103, No. EM4, Aug., 1977, pp. 527-535
22. Ziegler, H., "Modification of Prager's Hardening Rule", Quart., Appl. Math., Vol. 17, No. 1, 1959, pp. 56-65
23. Kent, D.C., and Park, R., "Flexural Members with Confined Concrete," Journal of the Structural Division, ASCE, Vol. 97, No. ST7, July, 1971, pp. 1969-1990
24. Sheikh, S.A., "Effectiveness of Rectangular Ties as Confinement Steel in Reinforced Concrete Columns," Department of Civil Engineering, University of Toronto, June, 1978
25. Manrique, M.A., Bertero, V.V., and Popov, E.P., "Mechanical Behavior of Lightweight Concrete Confined by Different Types of Lateral Reinforcement," University of California, Report No. UCB/EERC-79/05, May, 1979
26. Sargin, M., Ghosh, S.K., and Handa, V.K., "Effects of Lateral Reinforcement upon the Strength and Deformation Properties of Concrete," Magazine of Concrete Research, Vol. 23, No. 75-76, June-Sept., 1971, pp. 99-110
27. Burdette, E.G., and Hilsdorf, H.K., "Behavior of Laterally Reinforced Concrete Columns," ASCE, Vol. 97, No. ST2, Feb., 1971, pp. 587-602
28. Hisada, T., Ohmori, N., and Bessho, S., "Earthquake Design Considerations in Reinforced Concrete Columns," The Journal of the International Association for Earthquake Engineering, Vol. 1, No. 1, 1972, pp. 79-91